Severe Multiple Contingency Screening in Electric Power Systems

Vaibhav Donde, *Member, IEEE*, Vanessa López, Bernard Lesieutre, *Senior Member, IEEE*, Ali Pinar, *Member, IEEE*, Chao Yang, and Juan Meza

***Abstract*—We propose a computationally efficient approach to detect severe multiple contingencies. We pose a contingency analysis problem using a nonlinear optimization framework, which enables us to detect the fewest possible transmission line outages resulting in a system failure of specified severity, and to identify the most severe system failure caused by removing a specified number of transmission lines from service. Illustrations using a three-bus system and the IEEE 30-bus system aim to exhibit the effectiveness of the proposed approach.**

***Index Terms*—Load flow analysis, load shedding, optimization methods, power system reliability, power system security.**

I. Introduction

ROBUST operation of a power grid requires anticipation of unplanned component outages that could lead to dramatic and costly blackouts. Planning and operating criteria are designed in order that "the interconnected power system shall be operated at all times so that general system instability, uncontrolled separation, cascading outages, or voltage collapse, will not occur as a result of any single contingency or multiple contingencies of sufficiently high likelihood" [1]. Additional, more specific criteria help to achieve this famous $N-1$ criterion in practice. In this paper we consider the potential effects of the loss of multiple elements. Specifically, we pose the following two related optimization problems: 1) minimize the number of failure events that will necessitate a minimum amount of (specified) loss of load to maintain the integrity of the grid, and 2) calculate the maximum loss of load that would be required to survive a (specified) limited number of events, in any possible combination. For example, we could identify a minimum number of events that would require the loss of 1000 MW of load, or we might calculate the most load shedding (and location) for any $N-3$ scenario. We believe these "worst-case" analyses of the more general $N-k$ problem are interesting in their own right. They can provide planners and operators more confidence in the security of the system beyond the $N-1$ requirement. Furthermore we recognize that we now operate under conditions in which there is concern about the possibility of purposeful and malicious $N-k$ scenarios. Such concerns may be best addressed by identifying $N-k$ scenarios that have severe consequences.

In this paper we consider the problem in a static sense through the examination of operating points in relation to the feasibility boundary of the power flow equations. Analysis of the power flow feasibility boundary has received considerable attention in the literature. Most notably it has been widely studied in terms of the use of bifurcation theory to calculate margins for secure operation relative to voltage collapse and dynamic instability. Many articles discuss this general topic (see [6] and references therein, for an overview). The most relevant to the present work are those that calculate a minimum distance to the feasibility boundary from an operating point (for a fixed network topology) [3], [10], [11], [13], [21]. This past work has also established the geometrical interpretations of a direction of best load shedding strategy in the space of load powers. For instance, Alvarado *et al.* [3] computed the point on the feasibility boundary closest to the present operating point, that is, the minimum change in power injections that would result in operation at the edge of feasibility. This closest point on the feasibility boundary provided a measure of the security margin for the given network topology, and it provided the best direction for load shedding. Our approach is motivated by those interpretations. Moreover, we allow the network topology to change in order to incorporate transmission line failures.

Our primary contribution in this paper is to propose a method for identifying the fewest network topological changes (removal of transmission lines) that result in operating point infeasibility, such that the amount of minimum load shedding required for feasible operation is greater than a user-defined threshold. Thus we deal with changes in network topology and the operating point simultaneously within the same mathematical framework. The amount of required load shedding provides a measure of the severity of the event.

Since a static framework is used, the multiple contingencies we examine should be considered to occur simultaneously or in short succession, before the system is redispatched to a new operating point. Likewise the minimal load reduction suggested by our solutions would need to be affected quickly to avoid an even larger disturbance. Details of dynamic response, operator actions, and automatic controls are not modeled in this paper. Rather, we intend that the contingencies identified using our

Manuscript received June 29, 2006; revised August 30, 2007. This work was supported by the Director, Office of Science, Division of Mathematical, Information, and Computational Sciences of the U.S. Department of Energy under Contract DE-AC03-76SF00098. Paper no. TPWRS-00392-2006.

V. Donde is with ABB Corporate Research Center, Raleigh, NC 27606 USA (e-mail: vaibhav.d.donde@us.abb.com).

V. López is with IBM T. J. Watson Research Center, Yorktown Heights, NY 10598 USA (e-mail: lopezva@us.ibm.com).

B. Lesieutre is with University of Wisconsin-Madison, Madison, WI 53706 USA (work performed while at Lawrence Berkeley National Laboratory, CA) (e-mail: BCLesieutre@lbl.gov).

A. Pinar, C. Yang, and J. Meza are with the Computational Research Division, Lawrence Berkeley National Laboratory, Berkeley, CA 94720 USA (e-mail: APinar@lbl.gov; CYang@lbl.gov; JCMeza@lbl.gov).

Digital Object Identifier 10.1109/TPWRS.2008.919243

screening techniques will be used to define the scenarios for detailed dynamic studies. We note that the severity of the events identified could be different when dynamics are considered.

Mathematically, we work with a nonlinear optimization problem in terms of both network active and reactive powers and pose the problem as a mixed integer nonlinear optimization problem. Then we solve this problem through a two stage analysis. In the first stage, we force the feasibility boundary to move past the nominal operating point (rendering it infeasible) by a user-specified distance, through alterations to the network. A relaxation technique, similar to that used in [14], is employed to identify a small set of line outages that will contract the feasibility boundary by at least the required amount. This set of lines is further processed in the second stage. Detailed $N-k$ analysis is performed considering only subsets of the lines identified in the first stage. Given that such lines are typically few in number, the computational burden of the $N-k$ analysis in the second stage is far less than a complete analysis of all lines in the system.

A similar problem of multiple contingency identification has been addressed by other researchers. Salmeron *et al.* [22] employed a bilevel optimization framework along with mixed-integer linear programming to analyze the security of electric grids under terrorist threat. The critical elements of the grid were identified by maximizing the long-term disruption in the power system operation caused by terrorist attacks based upon limited offensive resources. The bilevel programming framework has also been used by Arroyo and Galiana [4]. In all these formulations the bilevel optimization framework appears promising at identifying critical system vulnerabilities.

We emphasize that we pursue a deterministic, worst-case framework because we would like to anticipate events that include those arising from malicious design. For a probabilistic approach to $N-k$ analysis for naturally occurring events, the reader may consider the stochastic approach proposed in [8].

The static collapse of power systems is closely associated with network topology. Our previous work [12] showed that an approximate power flow description provides a way to relate static collapse with graph partitioning using spectral graph theory. Grijalva and Sauer [16], [17] related topological cuts with the static collapse based on branch complex flows. He *et al.* [18] used a voltage stability margin index to identify weak locations in a power network. Although the connections of static collapse with graph theory are useful and interesting in their own right, they remain approximate and qualitative at this stage and are not discussed further in this paper.

II. Problem Description

Conceptually, we aim to identify a small set of transmission lines whose removal from service would minimally necessitate a reduction in load to avoid a potentially severe blackout. We consider the minimum load lost after the failure occurs to be the measure of the severity of the event. Thus, we pose the fundamental question: what is the least altered network topology that makes the power flow infeasible at the nominal load distribution, and for which the minimum amount of load required to be shed to make the power flow feasible again is greater than some specified severity threshold?

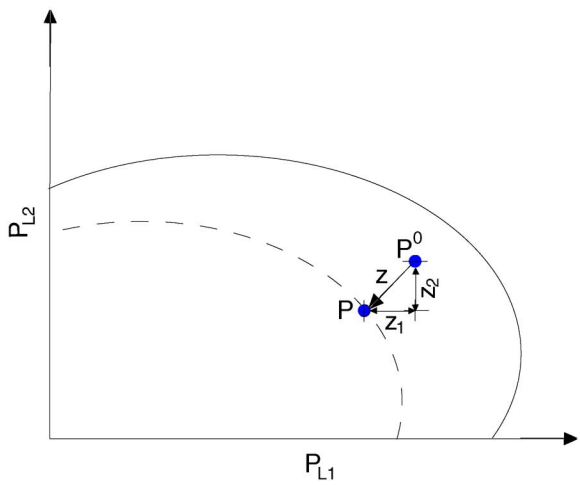

Fig. 1. Schematic view of load shedding process in the space of active load powers.

A schematic view of the load shedding process is provided in Fig. 1. The solid-lined curve represents the nominal power flow feasibility boundary when all the lines are in service. The nominal operating point P^0 lies within the feasible region of operation. When a few lines are removed from service, the feasible region shrinks and the boundary moves to the one shown as a dashed-line. The minimal load shedding strategy moves the original operating point P^0 to an operating point P that lies on the new feasibility boundary. The amount of the total load shedding, for instance, z_1+z_2, corresponds to a measure of severity. Note that the feasibility boundaries may be nonconvex in general, although they appear convex in the schematic representation shown in Fig. 1.

In our analysis we consider a lossless power system network having m buses (nodes) and n lines (branches). Let P and Q be, respectively, vectors whose components are given by the active and reactive power injections at the buses. Due to the lossless character of the system, we have $\sum_{i=1}^{m} P_i = 0$, however, $\sum_{i=1}^{m} Q_i > 0$ as part of the reactive power is consumed in the network.

It is natural to cast our problem as a mixed integer nonlinear programming (MINLP) problem, which is difficult to solve, in part due to the complexity and nonconvexity of the model, and in part because our decision variables are binary (a line is either in service, or not). In our mathematical description we define indicator variables $\gamma_i \in \{0,1\}$ to represent whether a line is in service: a value of $\gamma_i = 0$ is nominal and indicates that the line is in service. MINLP problems are notoriously hard to solve, and the general purpose tools are of limited availability. In this work, we use a continuous relaxation technique to show the validity of our models. Solving the MINLP formulation remains an important problem, and we are currently working on methods that can exploit the problem specific structure. However, these efforts are beyond the scope of this paper, and in this work, we first attempt to find an optimal solution to a relaxed problem in which the integer variables are allowed to take on continuous values, i.e., $\gamma_i \in [0,1]$. We allow this in the first stage of our screening algorithm. Then the relaxed solution is processed to

explore the nearby true integer solutions using a detailed model. We do this in the second stage of our screening.

It is interesting to note that this common relaxation procedure has an obvious interpretation in our power system model. Instead of the line being either in service, or out of service, the line admittance is allowed to vary between its nominal value and zero. While this appeals to our intuition, we caution the reader that there are important differences between a monitored line of any admittance, and the absence of that line which removes its constraint on the model. We view the relaxation used in the first stage as a technique for approaching this difficult integer optimization problem. It is appealing from a computational point of view, but might yield suboptimal results. In this paper, however, we will occasionally appeal to the reader's intuition in terms of reduced admittances.

The network angle variables and voltage magnitudes are denoted by vectors θ and V, respectively, and matrix B is a diagonal matrix of line susceptances.[1] The active and reactive power flow equations (with modified admittances) can be written in matrix form as

$$A^T EB(I-\Gamma)\sin(A\theta) = P \tag{1}$$

$$-|A|^T EB(I-\Gamma)\cos(A\theta) + d = Q \tag{2}$$

where A is the branch-node incidence matrix of the network graph. Each row of A contains a single entry equal to 1 and a single entry equal to -1, at locations corresponding to the terminal buses of the lines, and $|A|_{i,j} = |A_{i,j}|$. E is a diagonal matrix with

$$E_{i,i} = \exp((|A|\ln V)_i), \quad i = 1,\ldots,n$$

which simply evaluates to the product V_iV_j corresponding to a line connecting buses i and j. I is the identity matrix, Γ is a diagonal matrix with

$$\Gamma_{i,i} = \gamma_i, \quad i = 1,\ldots,n$$

d is defined by

$$d_i = V_i^2 \times (A^T B(I-\Gamma)A)_{i,i}, \quad i = 1,\ldots,m$$

and $\sin(A\theta)$ denotes a vector whose ith component is equal to $\sin((A\theta)_i)$. Similar notation is used to define $\cos(A\theta)$ and $\ln V$. This model form is chosen to highlight the topological information in the network incidence matrix A. Direct expansion of these expressions will yield the power flow equations in standard form. Refer to [9] and [23] for more details on this model.

Most work documented in the literature in this context assumes the notion of a slack bus. The choice of the slack bus is typically arbitrary and it often serves to supply network losses. Moreover, in the event of load shedding or load pick up, the slack bus is assumed to provide the net reduction or increment in the loads. It is well known, but often understated, that the results depend upon the choice of the slack bus. In this study, we use a *distributed slack bus*, where the net reduction in load due to load shedding is accounted for by every generator in the system lowering their respective dispatches in proportion to their generating capacities.[2] This eliminates the aspect of arbitrariness that the results contain when a particular bus is used as a slack bus. This choice of distributed slack is motivated by the presence of droop governor controls on generators in which the response to a disturbance is distributed in a uniform manner among the generators. In the WECC system, for example, generators have 5% droop governor controls [2].

We note that due to the incorporation of a single unified distributed slack mechanism in our framework, all the generators in the system are redispatched in proportion to their nominal dispatches in response to load shedding, even when line failures result in system islanding (disconnected groups or partitions). Multiple distributed slack mechanisms would be more appropriate while dealing with cases when there is partitioning of the graph underlying the system network. Such an approach can be easily followed once the partitioning details are known. However we note that the analysis presented in this paper does not explicitly address issues related to system islanding and graph partitioning. Finally we remark that, although the aforementioned distributed slack mechanism has been adopted for this study, the contingency screening approach we propose is general enough to allow the use of other distributed slacks or load redispatching mechanisms.

A. Power Flow Model, Load Shedding, and Distributed Slack

Suppose that the system has m_g PV (generator) buses and m_l PQ (load) buses, such that the total buses are $m = m_g + m_l$. Let ${P^0}_{pv}$ and ${P^0}_{pq}$ be the vectors of active power injections at PV and PQ buses, respectively, at the original operating point P^0. Let $z \in \mathbb{R}^{m_l}$ be a vector representing a reduction in the active load powers due to load shedding. In general, some PQ buses in the network will not have any load connected to them. In other words, such buses will have no load shedding activity associated with them. Corresponding components of the vector z are set to zero. It is assumed that the loads are constant power factor loads, so that the relationship ${Q^0}_{pq} = M{P^0}_{pq}$ holds, where ${Q^0}_{pq}$ represents a vector of reactive power injections at PQ buses and M is a diagonal matrix. Hence, the reduction in reactive load powers is equal to Mz. In the space of active load powers, the vector z provides a direction for load shedding, whose components are schematically represented in Fig. 1.

Note that all the elements of z are nonnegative; loads may decrease but not increase. Due to the adopted notion of a distributed slack bus and the lossless character of the network, the net reduction in the active power load due to load shedding, i.e., $e^T z$, where $e = [1\ 1\ \ldots\ 1]^T \in \mathbb{R}^{m_l}$, is accounted for by a reduction in generation at every PV bus. With our choice of distributed slack bus, the change in power at each generator is in

[1]It is assumed for simplicity that the lines are lossless and shunt elements are absent. However the mathematical framework and the formulations proposed in later sections do not require this assumption.

[2]The notion of a distributed slack has been used in other applications. See, for example, [7] and [24].

direct proportion to its nominal dispatch relative to the total dispatch. The net reduction in active power injections at PV buses is given by the product $kP^0{}_{pv}$, where k is a (nonpositive) scalar. It follows from the conservation of active power that we must have $e^T z + k e^T P^0{}_{pv} = 0$, therefore

$$k = -\frac{e^T z}{e^T P^0{}_{pv}}. \tag{3}$$

Finally, we assume here that generator voltage controls act to maintain voltage magnitudes at the PV buses at their nominal values; thus, one need only consider the reactive power equations in (2) corresponding to PQ buses. Then, using (1)–(2), the power flow description at the new operating point P that is achieved after load shedding is given by

$$F^P_{pv}(\theta, V, \gamma) - \left(P^0{}_{pv} + kP^0{}_{pv}\right) = 0 \tag{4}$$
$$F^P_{pq}(\theta, V, \gamma) - (P^0{}_{pq} + z) = 0 \tag{5}$$
$$F^Q_{pq}(\theta, V, \gamma) - M(P^0{}_{pq} + z) = 0 \tag{6}$$

where k is as in (3), $F^P_{pv}(\theta, V, \gamma)$ and $F^P_{pq}(\theta, V, \gamma)$ denote, respectively, the left-hand side from (1) corresponding to PV and PQ buses, and $F^Q_{pq}(\theta, V, \gamma)$ represents the left-hand side from (2) corresponding to PQ buses. For a given network topology, the system of equations (4)–(6) geometrically represents an m_l-manifold in the space of variables (θ, V, z).

We remark that no angle reference is provided in the power flow description (4)–(6). As a result, the power flow Jacobian

$$J = \left[\begin{array}{cc} \frac{\partial F}{\partial \theta} & \frac{\partial F}{\partial V} \end{array}\right] \tag{7}$$

has a *trivial* zero eigenvalue with $w_0 = [e^T \ \mathbf{0}^T]^T$ as the corresponding left eigenvector, where $e = [1 \ 1 \ \ldots \ 1]^T \in \mathbb{R}^m$, $w_0 \in \mathbb{R}^{m+m_l}$, and F denotes the left-hand side of (4)–(6). This is also apparent from the structure of (1)–(2) and the fact that the sum of the elements in each row of the incidence matrix A is equal to zero. Note that w_0 satisfies

$$\frac{\partial F}{\partial z}^T w_0 = 0. \tag{8}$$

B. Obtaining a (Locally) Best Load Shedding Strategy

Referring to Fig. 1, a best load shedding strategy is sought that moves the initial operating point P^0 to a new operating point P, such that a minimum amount of load is lost. Results in the literature related to this topic have employed a 2-norm notion of distance to a feasible operating point, see for example [5]. In practice, since our emphasis is on minimum load shedding, it is more appropriate to express our distance in a 1-norm sense. That is, we are more interested in the simple sum of lost load than the sum of squared lost load.

Typically the 2-norm measure is more amenable to mathematical analysis than the 1-norm; however, we argue that the 1-norm better characterizes our interests. It measures the total lost load, while the 2-norm measures a more abstract quantity equal to the sum of squares of lost load. Typically, the 1-norm introduces an aspect of non-smoothness in the analysis, and thus may increase the complexity of the problem. As mentioned in Section II-A, in the present case every load is only allowed to be shed as opposed to being increased. This requires all the elements of z to have the same sign, in particular they need to be all nonnegative in the present framework. This observation greatly reduces the complexity that the problem would encounter otherwise, and simplifies $\|z\|_1$ to $e^T z$ (which would otherwise be $e^T|z|$). To determine such a load shedding strategy, consider the following optimization problem

$$\min_{\theta, V, z} \quad e^T z \tag{9}$$
$$\text{s.t.} \quad F(\theta, V, z) = 0 \tag{10}$$
$$P^0_{pq} \le P^0_{pq} + z \le 0 \tag{11}$$
$$V_{\min} \le V \le V_{\max} \tag{12}$$
$$-\pi/2 \le A\theta \le \pi/2 \tag{13}$$

where (10) denotes the system (4)–(6) for a given network topology (i.e., for fixed γ), such that it does not have a solution at $z = 0$. Inequality constraints (11)–(13) ensure that the variables are within bounds. Note, in particular, that (11) ensures the validity of this formulation by enforcing nonnegativity of elements of vector z. It also ensures that the upper limit on the amount of load shedding is defined by the nominal load, thus preventing the loads to act as generators. Voltage magnitudes at PQ buses are bounded by upper and lower limits $V_{\max}$ and $V_{\min}$, respectively, as indicated by (12). This constraint ensures that the voltages are within acceptable limits, even after load shedding. With a good choice of $V_{\min}$, this constraint also serves to exclude low voltage (steady state unstable) solutions from consideration. Constraint (13) guarantees that the phase angles across the transmission lines are in a range acceptable for a steady state stable operation of the power system.

The Lagrangian corresponding to (9)–(13) is

$$\begin{aligned}\mathcal{L} = {} & z^T e + \lambda^T F(\theta, V, z) + \mu_1^T(-z) + \mu_2^T\left(P^0_{pq} + z\right) \\ & + \mu_3^T(V_{\min} - V) + \mu_4^T(V - V_{\max}) \\ & + \mu_5^T(-\pi/2 - A\theta) + \mu_6^T(A\theta - \pi/2)\end{aligned} \tag{14}$$

where λ and $\mu_1, \ldots, \mu_6$ are vectors of Lagrange multipliers. Optimal solutions to this problem satisfy the following Karush–Kuhn–Tucker conditions

$$e + \frac{\partial F}{\partial z}^T \lambda - \mu_1 + \mu_2 = 0 \tag{15}$$
$$J^T\lambda + \begin{bmatrix} -A^T\mu_5 + A^T\mu_6 \\ -\mu_3 + \mu_4 \end{bmatrix} = 0 \tag{16}$$
$$\mu_1 \cdot z = 0 \tag{17}$$
$$\mu_2 \cdot (P^0_{pq} + z) = 0 \tag{18}$$
$$\mu_3 \cdot (V_{\min} - V) = 0 \tag{19}$$
$$\mu_4 \cdot (V - V_{\max}) = 0 \tag{20}$$
$$\mu_5 \cdot (\pi/2 + A\theta) = 0 \tag{21}$$
$$\mu_6 \cdot (A\theta - \pi/2) = 0 \tag{22}$$
$$\mu_1, \ldots, \mu_6 \ge 0 \tag{23}$$

along with (10)–(13). Thus the vector z that provides the best load shedding strategy is obtained by solving (10) and (15)–(22), while satisfying the inequalities (11)–(13) and (23). The notation "$\cdot$" in (17)–(22) is used to indicate component-wise multiplication of associated vectors.

When the inequality constraints (11)–(13) are inactive, we have $\mu_1, \ldots, \mu_6 = 0$. Referring to (16), this results in $J^T\lambda = 0$, which in turn makes λ a left eigenvector of J corresponding to its zero eigenvalue. Note that J must have an extra (nontrivial) zero eigenvalue, as $\lambda = w_0 = e^T$ does not satisfy (15) and (8) simultaneously. In other words, λ equals w, where w is a left eigenvector of J corresponding to its nontrivial zero eigenvalue. For this case, it is insightful to appreciate the geometrical interpretation of (15)–(16). Consider a hyperplane tangent to the manifold defined by (10). Vectors $(\delta\theta, \delta V, \delta z)$ on that tangent hyperplane satisfy

$$J\begin{bmatrix}\delta\theta\\ \delta V\end{bmatrix} + \frac{\partial F}{\partial z}\delta z = 0. \tag{24}$$

Premultiplying with the eigenvector w^T results in

$$w^T J\begin{bmatrix}\delta\theta\\ \delta V\end{bmatrix} + w^T\frac{\partial F}{\partial z}^T \delta z = 0. \tag{25}$$

However, as the first term in (25) vanishes to zero, we must have $((\partial F)/(\partial z)w)^T\delta z = 0$. This implies that the normal to the power flow feasibility boundary at (θ, V, z) is given by $(\partial F)/(\partial z)^T w$. It also follows from (15) that this normal aligns with e when the inequality constraints are inactive.

C. Constrained Optimization Problem

Our formulation of the contingency screening problem employs the mechanisms of best load shedding strategy, distributed slack and binary line indicator variables, described in the previous sections. Note that we seek to move both the original operating point P^0 and the power flow feasibility boundary. This boundary is moved past P^0 such that the minimum load shedding required to move P^0 to a different operating point lying on the new boundary is greater than the minimum desired severity of the blackout. Mathematically, the problem takes the following form:

$$\min_{\theta,V,z,\gamma,\mu_1,\ldots,\mu_6,\lambda} \quad e^T\gamma \tag{26}$$

$$\text{s.t.} \quad F(\theta, V, z, \gamma) = 0 \tag{27}$$

$$e + \frac{\partial F}{\partial z}^T \lambda - \mu_1 + \mu_2 = 0 \tag{28}$$

$$J^T\lambda + \begin{bmatrix}-A^T\mu_5 + A^T\mu_6\\ -\mu_3 + \mu_4\end{bmatrix} = 0 \tag{29}$$

$$\mu_1 \cdot z = 0 \tag{30}$$

$$\mu_2 \cdot \left(P^0_{pq} + z\right) = 0 \tag{31}$$

$$\mu_3 \cdot (V_{\min} - V) = 0 \tag{32}$$

$$\mu_4 \cdot (V - V_{\max}) = 0 \tag{33}$$

$$\mu_5 \cdot (\pi/2 + A\theta) = 0 \tag{34}$$

$$\mu_6 \cdot (A\theta - \pi/2) = 0 \tag{35}$$

$$\mu_1, \ldots, \mu_6 \geq 0 \tag{36}$$

$$P^0_{pq} \leq P^0_{pq} + z \leq 0 \tag{37}$$

$$V_{\min} \leq V \leq V_{\max} \tag{38}$$

$$-\pi/2 \leq A\theta \leq \pi/2 \tag{39}$$

$$\gamma \in \{0, 1\} \tag{40}$$

$$e^T z \geq S_{\min}. \tag{41}$$

Constraints (27) denotes the power flow equations (10), now with γ as an additional variable. Together, constraints (27)–(39) are the Karush–Kuhn–Tucker conditions as obtained in Section II-B; they are repeated here for clarity. These constraints help us avoid explicitly solving a bilevel optimization problem. Constraint (40) limits γ variables to binary values. Constraint (41) ensures the total amount of load shed is greater than $S_{\min}$, a positive-valued user-defined parameter that indicates the minimum severity of lost load.

By virtue of the distributed slack mechanism, all the generators contribute to the load shedding in the same proportion. This ensures that all the generators must reduce (not increase) their dispatches to account for load shedding, thus in turn ensuring that their upper dispatch capacity limits are never hit. This also guarantees that all generators will reach the lower dispatching limit (assumed as zero) simultaneously, when all the load in the system is shed. Thus a constraint that limits generator dispatches is not included in the set of constraints (27)–(41). Note, however, that if the lower dispatching limits are nonzero, constraints enforcing such limits can be added to the set (27)–(41). If we denote the minimum generation capacity of the ith PV bus by $(P^0_{\text{pv,min}})_i$, then the new generations would need to satisfy [cf. (4)]

$$\left(P^0{}_{pv}\right)_i + k\left(P^0{}_{pv}\right)_i \geq \left(P^0_{pv,\min}\right)_i \tag{42}$$

$i = 1, \ldots, m_g$. Using the definition of the scalar k given by (3) in (42), it follows that the constraints to enforce the lower dispatching limits would be

$$e^T z \leq \left(\frac{1 - \left(P^0_{pv,\min}\right)_i}{\left(P^0{}_{pv}\right)_i}\right) e^T P^0{}_{pv} \tag{43}$$

$i = 1, \ldots, m_g$. Note that only one such constraint would really need to be enforced, namely that for which $(1 - (P^0_{\text{pv,min}})_i/(P^0{}_{pv})_i)$ is smallest, since the remaining would then be necessarily satisfied. Moreover, when the generator corresponding to that constraint reaches its lowest capacity limit during optimization iterations, it is excluded from the distributed slack formulation (3), thus providing the freedom required for rest of the generators to participate in further load shedding. This can be achieved by placing an outer loop on the optimization problem (26)–(41) that gets activated when a generator lower dispatch limit given by (43) is reached and reinitializes the problem with the modified slack, that excludes the binding generator. Recall that our goal is to *quickly* screen multiple contingencies to identify the severe ones. A reasonably flexible and practical slack mechanism as the one we adopt, is sufficient to serve our goal.

In the present formulation, we aim to minimize the line outages (sum or indicator variables) that result in a failure having severity greater than $S_{\min}$. Another related formulation that can address our network vulnerability problem is where one aims to find the maximum possible failure severity when at most $L_{\max}$ number of lines are removed from service. Although both these formulations carry the same conceptual flavor, they are different problemsdepending on the values that the user defined parameters $S_{\min}$ and $L_{\max}$ take. Mathematically, the latter formulation has the same structure as (26)–(41), except that the objective is now replaced by

$$\max_{\theta,V,z,\gamma,\mu_1,\ldots,\mu_6,\lambda} \quad e^T z \tag{44}$$

and the constraint (41) is replaced by

$$e^T \gamma \leq L_{\max}. \tag{45}$$

while keeping other constraints intact.

D. Relaxation of Indicator Variables

The formulation in (26)–(41) is an MINLP problem, which is known to be a very hard problem to solve. General purpose MINLP solvers are only of limited availability and remain as research projects. In this work, we use a continuous relaxation technique, where we replace the binary line indicator variables with continuous variables in the [0,1] range. In other words, we allow partial line outages by letting

$$\gamma_i \in [0,1], \quad i = 1, \ldots, n. \tag{46}$$

The drawback of the relaxation technique is that the optimal solution to the continuous problem can be far away from the optimal solution to the discrete problem. Even when they are close, mapping the continuous solution to a feasible discrete solution may be a challenge. This drawback, however, has a silver lining for the contingency screening problem. For contingency screening, it would be preferable to provide a list of system weaknesses, as opposed to a single weakness. For instance, if any three broken lines out of a group of five lines might cause a blackout, it would be more valuable to detect the group of five lines instead of detecting the three-line combination that causes the most severe blackout. As we discuss later, continuous relaxation tends to identify these groups of lines. It is still important to develop algorithms to solve the MINLP formulation in (26)–(41), however the relaxation method employed in this paper validates the effectiveness of our proposed model.

Note that the discussion on obtaining the best load shedding strategy as in Section II-B is applicable for any fixed network topology (as long as the network remains connected). Thus it holds valid for the model with continuous variables. Using either formulation (26)–(41) or (44)–(45) with the integrality constraint relaxed, in the first stage of the screening process the critical lines for system security are identified as the ones that have non-zero γ's associated with them. In the second stage of our analysis, only such lines are considered for a detailed $N - k$ study, where N is the number of lines identified and k may take values from 1 through N. In this second stage the indicator variables are not relaxed; they take on true integer values.

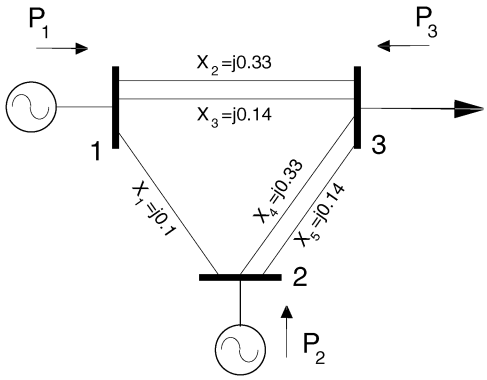

Fig. 2. Three-bus system.

Here it is appropriate to comment on the range of values for the relaxed indicator variables that may be expected during the first stage identification analysis. In particular, we would like to be sure that nonzero values are meaningful in some sense, and that spurious and confusing values do not occur. In formulation (26)–(41) we note that the sum of the values are minimized, and if changing a line's status does not contribute to satisfying the constraints, the optimization will tend to make the values identically zero. This is what we observe. In the 30-bus, 41-line example we consider later, we note that the solution for the indicator vector comprises 38 elements exactly equal to zero, one element exactly equal to 1.0, and two elements with values close to 1.0 (namely, 0.99 and 0.83). Somewhat in contrast, the formulation (44)–(45) does not directly minimize the sum of indicator vector values; the sum is specified in a constraint. In some cases it is possible that unimportant lines may be indicated by nonzero values. For example, if we pose the problem of finding the most severe N-3 event and this event is actually equivalent to an N-2 event (i.e., there is no N-3 event more severe than a particular N-2 event), then the two critical lines will be clearly identified, but there may be other lines erroneously identified with nonzero indicator values. In this latter formulation, some judgment is required: the higher-valued indicator variables indicate the most important lines.

III. Examples

To illustrate the application of the ideas discussed in Section II, we first consider a three-bus system (Fig. 2), followed by the IEEE 30-bus system (Fig. 7).

A. Three-Bus System

This small system is convenient for an easy graphical visualization of results and to highlight the main aspects of our formulation. Consider the network shown in Fig. 2, which has two generators and a single constant power factor load. The network data and the nominal power flow solution are summarized in Table VI.

Fig. 3 shows the space of active power injections at buses 2 and 3. Given that the system is lossless, the power injection at

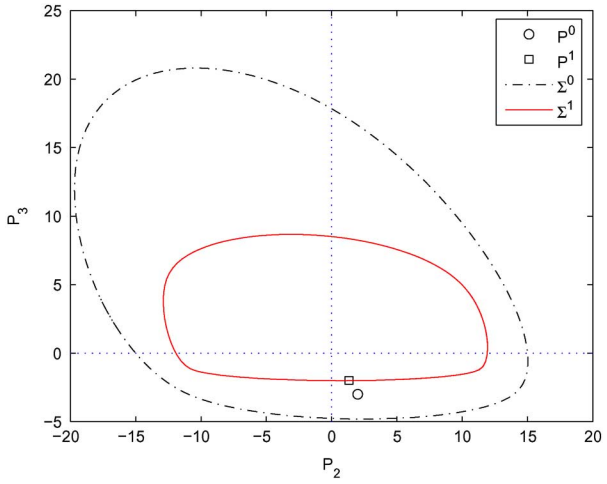

Fig. 3. Three-bus system: nominal and modified power flow solution space boundary as defined by the solution in Table I.

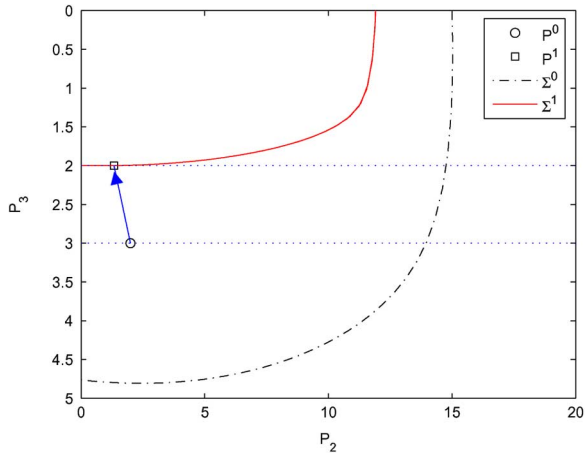

Fig. 4. Fourth quadrant of Fig. 3.

TABLE I
THREE-BUS SYSTEM SOLUTION: USING THE FORMULATION (26)–(41)

Lines identified		Load shed and generation redispatch		
Line #	γ	Bus #	P^0	P^1
3	0.67	1	1.0000	0.6667
5	1.00	2	2.0000	1.3333
		3	-3.0000	-2.0000

bus 1 is simply $-(P_2 + P_3)$ and consideration of another axis P_1 is unnecessary. When all the lines are in service, the power flow solution space boundary can be traced by a continuation technique [19] and is identified as Σ^0. The region enclosed by Σ^0 contains all possible power flow solutions that the present network topology (defined by line parameters) supports. The part of this region relevant to us is the quadrant having $P_2 \geq 0$ and $P_3 \leq 0$, given that the devices connected to buses 2 and 3 are a generator and load, respectively. Note that the nominal operating point P^0 lies within this region.

First we perform our analysis by avoiding voltage constraints, setting $V_{\min} = 0.5$ p.u. We then raise the limit to examine the effect of a binding voltage constraint. The generator buses 1 and 2 maintain voltages at 1.0 p.u., and no maximum voltage constraints are included (or would be needed).

Using the problem formulation (26)–(41), a few critical lines in this system are identified while ensuring that their removal will cause a failure having a severity of at least 1 p.u., or equivalently an event that will necessitate at least 1 p.u. of load shedding at bus 3. The corresponding parameter $S_{\min}$ is defined as 1. The initial guess for the solution process was obtained as described in Appendix B. The nonzero values of γ_3 and γ_5 in the solution, summarized in Table I, identifies lines 3 and 5 as important. The values for γ_1, γ_2, and γ_4 are identically zero.

The first-stage relaxation solution using the values for γ_3 and γ_5 shown in Table I, yield a load bus voltage of 0.55 p.u.; the phase angles across the lines (that still remain in service) are within $\pm\pi/2$. With both voltage and angle constraints (38)–(39) inactive, the power flow Jacobian J is nontrivially singular, as discussed in Section II-B. This is shown pictorially in Fig. 3. With the new network topology, the original boundary Σ^0 moves to Σ^1. Note that the original operating point P^0 lies outside this new boundary, and is now infeasible. The solution identifies point P^1 which achieves feasibility again by shedding the least possible load at bus 3. As the power flow Jacobian J is nontrivially singular, this point lies on Σ^1.

For clarity, the relevant (fourth) quadrant of Fig. 3 is redrawn in Fig. 4. The arrow represents the movement of the operating point from P^0 to P^1. Its projection onto the P_3 axis corresponds to the amount of load that is shed at bus 3. Note in Table I that due to the distributed slack bus mechanism, the generators have been redispatched in a constant proportion to their nominal values so as to accommodate the reduction of load at bus 3.

This first stage solution gives a severity of minimum lost load equal to 1.0 p.u. The second stage analysis is performed by removing both line 3 and line 5 from service. The resulting severity is 1.5582 p.u.

Now we use formulation (44)–(45) to maximize the severity while limiting the number of line outages to be no more than two (i.e., with $L_{\max} = 2$). The values for γ obtained by the optimization algorithm again identify lines 3 and 5 as the most important. To obtain this solution, which is summarized in Table II, the same initialization procedure as before is employed. The load bus voltage is again about 0.55 p.u. The optimization algorithm completely removes lines 3 and 5 from service in order to achieve the maximum of the objective function. (The values of γ for the other three lines are identically zero.) This corresponds to a severity of 1.5582 p.u. load shed at bus 3. Since this first stage analysis resulted in an integer only solution and no phase angle limits were reached, the second stage analysis is not required.

The voltage and angle constraints are inactive for this solution too, thus making the Jacobian J nontrivially singular. It follows that the new (post load shedding) operating point P^2, as identified in Fig. 5, lies on the power flow solution space boundary Σ^2 resulting from a complete removal of lines 3 and 5 from service. The operating points P^0 and P^1, and corresponding boundaries Σ^0 and Σ^1 are also shown for comparison. Note that first stage

TABLE II
THREE-BUS SYSTEM SOLUTION: USING THE FORMULATION (44)–(45)

Lines identified		Load shed and generation redispatch		
Line #	γ	Bus #	P^0	P^1
3	1.00	1	1.0000	0.4806
5	1.00	2	2.0000	0.9612
		3	-3.0000	-1.4418

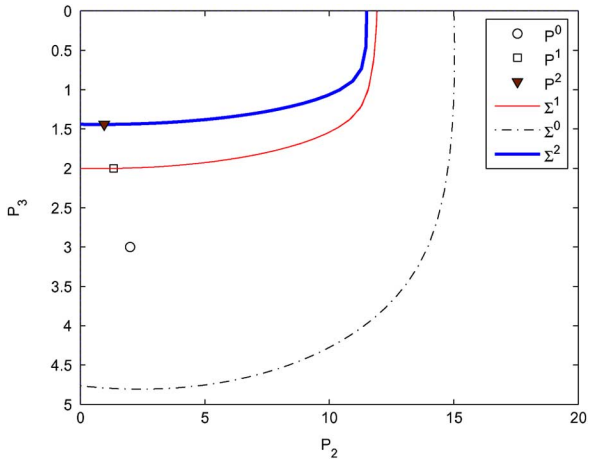

Fig. 5. Three-bus system: nominal and modified power flow solution space boundary as defined by the solution in Table II.

TABLE III
THE N − 2 ENUMERATION WITH THE THREE-BUS SYSTEM

Lines removed	Severity (Load shed at bus 3)	
	p.u.	% of nominal
1, 5	0.5120	17.07%
2, 3	0.5970	19.90%
2, 5	0.6000	20.00%
3, 4	0.5970	19.90%
3, 5	1.5582	51.94%
4, 5	0.5970	19.90%

relaxed solution for formulation (44)–(45) resulted in a higher value for γ_3, than for formulation (26)–(41). Correspondingly, the feasibility boundary Σ_2 is smaller than Σ_1, and more load is shed to reach Σ_2. Also note that the points P^0, P^1 and P^2 are collinear due to the incorporation of the distributed slack mechanism. That is, for instance, P^2 lies on Σ^2 as well as on the line joining P^0 and the origin.

In summary, the algorithms aim to identify a few line failures that will result in a significant loss of load. A direct $N-2$ analysis by enumeration, which is easy on this small system, is used to validate the results obtained above. Table III enumerates the cases where any two lines are removed from service such that the power flow is infeasible. Other combinations of two simultaneous line failures do not lead to power flow infeasibility, and they are not included in the table. The least amount of load shedding required to regain feasibility is also listed in each case. Note

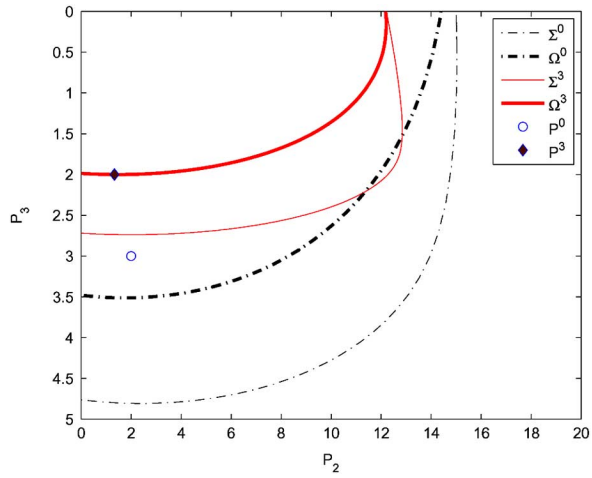

Fig. 6. Three-bus system: nominal and modified power flow solution space boundary, load bus voltage constraint boundary, and optimization solution.

that the removal of lines 3 and 5 achieves the highest possible severity.

We complete this analysis of the simple three-bus system by considering the effect of a binding voltage constraint. When $V_{\min}$ is set to 0.8 p.u., solutions to both the optimization formulations observe a binding lower voltage constraint (38), when other parameters are set as $S_{\min} = 1$ p.u. and $L_{\max} = 2$. Then at the solutions, the power flow Jacobian J is only trivially singular and the new (post load shedding) operating point does not lie on the power flow solution space boundary. Instead it lies on the manifold defined by $V_3 = V_{\min}$. Such a solution obtained using formulation (26)–(41) is depicted graphically in Fig. 6. Curve Ω^0 defines a boundary of the region where $V_3 > V_{\min}$, when all lines are in service (nominal case). This region is a subset of the complete power flow solution space, whose boundary is shown as Σ^0. The optimization formulation identifies lines 3 and 5, with their relaxation parameters as $\gamma_3 = 1$ and $\gamma_5 = 0.23$. Using these values, Σ^0 moves to Σ^3, and Ω^0 to Ω^3. The boundary Ω^3 encloses solutions having $V_3 > V_{\min}$, at this network topology. The optimization identifies the new operating point P^3 that lies on Ω^3, thus making sure that the voltage constraint is not violated, and yet at least 1 p.u. load is shed. (In this first stage relaxation formulation, exactly 1 p.u. load is shed.)

In this three-bus system, no single line failure contingency results in an infeasible operation. The second stage analysis simply calculates the severity of minimum lost load when both lines 3 and 5 are removed from service, while enforcing the voltage constraint. This severity is 1.95 p.u.

B. IEEE 30-Bus System

The IEEE 30-bus system as shown in Fig. 7 is considered for the identification of lines critical for system security using the formulation discussed in Section II-C. The generators are dispatched in the original system data [28] in such a way that the system observes an active power balance within the left, right and the lower parts of the network. To emphasize some important aspects of our algorithm, the generator active power injections are modified so that there is no natural power balance in

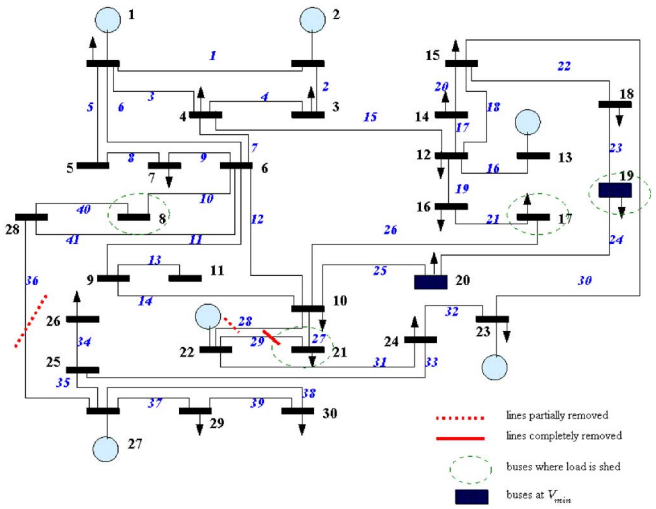

Fig. 7. Optimization solution for the IEEE 30-bus system.

the system subsets. Table VII documents the system data that are used to obtain the results that follow.

Problem formulation (26)–(41) is used for the contingency screening. Feasible initial guesses were obtained according to the procedure described in Appendix B. The solutions were computed using the solver SNOPT [15], the AMPL modeling language [25], and the NEOS server for optimization [26], [27]. SNOPT uses a sequential quadratic programming algorithm suitable for problems with (nonlinear) objective function and is designed for both nonlinear and linear constraints with sparse derivatives. The latter is particularly attractive for the optimization problem under consideration. The number of iterations taken by SNOPT to solve the problem varied between 50 and 1000, whereas the number of objective function evaluations and gradient/Jacobian evaluations ranged from 5 to 272 and 4 to 271, respectively. Since the problem is nonlinear, the performance of a solver is dependent in part by the initial guess supplied, and hence the ranges in the number of iterations and function evaluations for different runs.

An obvious (and trivial) solution to the optimization problem is the one that isolates all the generation from the loads, by removing radial lines that connect generators (and/or loads) with rest of the system. Such cases are excluded by not allowing the radial lines (in this case, lines 13, 16 and 34) to be removed from service, as our goal is to identify more subtle solutions than those trivially revealed in the network topology.

Buses having generators attached to them are assumed to have 1.05 p.u. voltage. The base case (all lines in service and no load shedding) power flow solution results in a voltage profile such that the lowest bus voltage in the system is 0.92 p.u. (at bus 8). Within the optimization framework, the post contingency limit of $V_{\min} = 0.8$ p.u. is enforced on load bus voltages. This limit is chosen because reliability criteria do not allow lengthy voltage dips below 80% of nominal [1]. Also, we expect that either automatic controls or operator action will quickly restore voltages to nominal levels.

Fig. 7 depicts a first stage relaxation solution based upon an initial guess provided by the initialization procedure described in Appendix B. The parameter $S_{\min}$ was set to 2 p.u. This

TABLE IV
IEEE 30-BUS SYSTEM SOLUTION

Lines identified		Load shed			Buses
Line #	γ	Bus #	p.u.	% of nominal	at V_{min}
28	0.99	8	0.2131	14.2%	19, 20
29	1.00	17	0.4500	100.0%	
36	0.83	19	0.4619	97.2%	
		21	0.8750	100.0%	

TABLE V
SELECTED ENUMERATION WITH THE IEEE 30-BUS SYSTEM

Lines removed	Severity p.u.	Load shed			Buses
		Bus #	p.u.	% of nominal	at V_{min}
28, 29	1.2431	17	0.1296	28.8%	17, 19
		19	0.2418	50.9%	
		21	0.8717	99.6%	
29, 36	0.2596	21	0.2596	29.7%	21
28, 29, 36	2.3413	8	0.2501	16.7%	18
		10	0.1812	62.5%	
		17	0.4500	100.0%	
		19	0.4750	100.0%	
		20	0.1100	100.0%	
		21	0.8750	100.0%	

amounts to shedding at least 24.4% of the total load in the system. This solution identifies three transmission lines as critical ones. (The remaining lines have corresponding values of γ equal to zero.) Table IV summarizes this solution. Using the values of γ_{28}, γ_{29}, and γ_{36} provided in this table, the generation rich lower region of the network is almost unable to supply loads in the other regions. This results in a sagging voltage at buses 19 and 20, and they are constrained at $V_{\min}$. Effectively, as the solution identifies, loads at this bus and neighboring buses must be shed to maintain power flow and voltage feasibility.

Having identified three lines in the first stage analysis, we now perform the second stage $N - k$ study by only considering these lines (where N is now 3, rather than 41). Note that the computational burden reduces drastically, for instance, the number of combinations to analyze reduce from 820 to 3 combinations for the $N - 2$ study. Table V describes the results of such an enumeration process, along with the load shedding to be performed at various buses to just avoid the otherwise impending system failure. The third column of Table V provides a load shedding strategy that will just avoid the infeasibility caused by the line removals. The net load reduction due to the load shedding is accounted for by the distributed slack mechanism. Mathematically, the process of identifying such a load shedding strategy corresponds to solving the optimization problem (9)–(13), with the constraint (13) enforced only on the lines in service.

Referring to Table V, the removal of lines 28 and 29 lead to an infeasible operation. The total of 1.2431 p.u. load at buses 17, 19 and 21 must be shed in order to maintain feasibility. This load shedding would place the voltage at buses 17 and 19 at

$V_{\min}$. The system operation is also infeasible when lines 29 and 36 are removed from service. A total of 0.2596 p.u. load must be shed to maintain feasibility. Voltage at the bus 21 would be at $V_{\min}$ when this load shedding is executed.

When all the identified lines, namely, lines 28, 29 and 36 are removed from service at a time (Table V, last row), the system gets grouped into two subsystems that are connected to each other by a single line (line 30). Recall that the group at the lower part of the network is generation rich. This results in a substantial need for load shedding in the other group (2.3413 p.u., which is 28.5% of the total system load). Even with all the load at buses 17, 19, 20 and 21 being shed along with partial load shedding at buses 8 and 10, the voltage at bus 18 would be as low as $V_{\min}$.

IV. Conclusion

In this paper, we propose a computationally feasible approach to detect multiple contingencies resulting in a severe system failure that does not require a prohibitively expensive enumeration. This approach provides an avenue to undertake a higher order $N-k$ security analysis on a large-scale power system.

Our approach seeks to identify a few line outages such that the system will need to shed significant amount of load in order to continue a feasible operation. It is important to discuss the level of modeling detail we have used and the impact it may have on results. By incorporating a nonlinear power flow, a droop-governor-motivated distributed slack bus, and using a one-norm metric, our model is consistent with (or is more detailed than) the models used in the most closely related literature on calculating the distance to the power flow feasibility boundary. Nevertheless, it lacks a detailed representation of system dynamics and therefore our results may be optimistic if the system were to exhibit instabilities. Alternatively, neglecting fast-acting reserves and special remedial action schemes that may be in place, may make our results pessimistic. We will work in the future to add some of these features to our model. We believe the model is valuable in its present form for identifying multiple contingencies that may undergo further scrutiny, perhaps with a detailed dynamic model.

We should also comment on the practical algorithms to perform the computations outlined in this paper. While the results on our test systems reveal the effectiveness of the problem formulation, the associated nonlinear optimization problem offers many challenges for larger (continental size) problems. Due to the nonlinearity of power flow equations and other constraints, the resulting optimization problem is in general nonconvex. Thus the solution obtained corresponds to a local optimum, depending upon the initial guess, the solver used and complexity of the power network under consideration. We have posed our problem in a worst-case optimization framework, but the nonconvexity inherent in the model suggests that we cannot prove the result is indeed the worst case result. We would like to point out that this issue of nonconvexity applies to all optimization problems that use a nonlinear model for the power grid, including traditional economic-focused optimal power flows, security margin calculations, etc., although one rarely encounters this caveat mentioned in the literature. (See [20] for a discussion of the impact of nonconvexity in the context of electricity markets.)

TABLE VI
Three-Bus System Data (Nominal Power Flow)

Bus data					Line data	
Bus #	P inject. (net), p.u.	Q inject. (net), p.u.	Ang., θ rad	Volt., V p.u.	Line #	React. X, p.u.
1	1.0000	1.7040	0.0420	1.0000	1	0.10
2	2.0000	1.7600	0.0770	1.0000	2	0.33
3	-3.0000	-2.4000	-0.1200	0.8412	3	0.14
					4	0.33
					5	0.14

The advantage of studying the test systems presented in this paper is that the results up to $N-2$ can be verified by complete enumeration. The removal of lines 28 and 29 that we identify as the worst $N-2$ case in the IEEE 30-bus example is confirmed by complete enumeration of all possible 2-line outages (excluding the ones that result in system islanding). Our approach for determining initial guesses, outlined in Appendix B, has worked well so far, but we will need to keep the issue of nonconvexity in mind as we develop algorithms for large-scale systems. Special algorithms need to be developed since commercial power flows do not presently perform the calculations we have developed here. The state of the art in high performance computing provides a platform to efficiently deal with large, complex and nonconvex problems. We are currently working on algorithms that can efficiently exploit such platforms.

Appendix A
Example System Data

This appendix summarizes the data used for the three-bus system and the IEEE 30-bus system, used in this paper. Tables VI and VII include the network parameters and the nominal power flow solution for these two systems respectively. Note that a few PV buses in the 30-bus system have local loads connected. Such buses are considered as PV buses with the nominal generation as the net nominal injection. In other words, they are assumed to not have any ability to perform load shedding. However a slight modification to (4)–(6) can handle the shedding of loads local to their generation.

Appendix B
Obtaining Feasible Initial Guesses

Nonconvexity of the optimization formulation (26)–(41) demands good (feasible) initial guesses to obtain convergence. Such initial guesses can be obtained by using simplified problem formulations of the main problem. One such approach is outlined here and is used to obtain the solutions discussed in Sections III-A and B.

Authors discuss in [12] that the problem of contingency screening can be formulated using spectral graph partitioning approach and simplified power flow. In that formulation, all the bus voltages are assumed to be at 1 p.u., however the nonlinearity in terms of the angles is fully considered. Solutions obtained using that approach can be processed further

TABLE VII
IEEE 30-BUS SYSTEM DATA (NOMINAL POWER FLOW)

Bus data					Line data	
Bus #	P inject. (net), p.u.	Q inject. (net), p.u.	Ang., θ rad	Volt., V p.u.	Line #	React. X, p.u.
1	0.1765	0.5084	0.0438	1.0500	1	0.06
2	0.9635	2.0656	0.0441	1.0500	2	0.19
3	-0.1200	-0.0600	0.0102	0.9837	3	0.17
4	-0.3800	-0.0800	0.0075	0.9723	4	0.04
5	0.0000	0.0000	-0.0330	0.9740	5	0.20
6	0.0000	0.0000	-0.0178	0.9530	6	0.18
7	-1.1400	-0.5450	-0.0851	0.9314	7	0.04
8	-1.5000	-0.7500	-0.0685	0.9233	8	0.12
9	0.0000	0.0000	0.0362	0.9759	9	0.08
10	-0.2900	-0.1000	0.0634	0.9890	10	0.04
11	0.0000	0.0000	0.0362	0.9759	11	0.21
12	-0.5600	-0.3750	0.2017	0.9472	12	0.56
13	2.1000	1.2760	0.5018	1.0500	13	0.21
14	-0.3100	-0.0800	0.1444	0.9414	14	0.11
15	-0.4100	-0.1250	0.1697	0.9554	15	0.26
16	-0.1750	-0.0900	0.1032	0.9398	16	0.14
17	-0.4500	-0.2900	0.0476	0.9568	17	0.26
18	-0.1600	-0.0450	0.0468	0.9320	18	0.13
19	-0.4750	-0.1700	-0.0037	0.9300	19	0.20
20	-0.1100	-0.0350	0.0074	0.9423	20	0.20
21	-0.8750	-0.5600	0.1059	1.0280	21	0.19
22	1.5795	2.1958	0.1335	1.0500	22	0.22
23	1.3000	0.8515	0.3294	1.0500	23	0.13
24	-0.4350	-0.3350	0.2010	1.0084	24	0.07
25	0.0000	0.0000	0.3076	1.0115	25	0.21
26	-0.1750	-0.1150	0.2394	0.9638	26	0.08
27	2.0955	1.1650	0.4075	1.0500	27	0.07
28	0.0000	0.0000	0.0193	0.9476	28	0.15
29	-0.1200	-0.0450	0.2871	1.0050	29	0.02
30	-0.5300	-0.0950	0.2047	0.9884	30	0.20
					31	0.18
					32	0.27
					33	0.33
					34	0.38
					35	0.21
					36	0.40
					37	0.42
					38	0.60
					39	0.45
					40	0.20
					41	0.06

to provide feasible initial guesses to the optimization problem (26)–(41), as discussed below.

One can note just by inspection of the three-bus system that the most severe blackout is obtained by removing lines 2–5 from the network as it will isolate the load from generation. Such a situation can be systematically identified by the graph theory based algorithm discussed in [12] for a larger system. For example, a significant blackout is obtained by removing lines 28, 29, 30 and 36 for the IEEE 30-bus system, as identified in [12]. By allowing the line parameter γ associated with only these lines to vary, the initialization process poses the problem: what is the most (locally) severe failure that can be obtained by partially removing only these lines from service? This problem can be described mathematically in an optimization framework as

$$\max_{\theta,V,z,\gamma,\mu_1,\ldots,\mu_6,\lambda} \quad e^T z \tag{47}$$

such that constraints (10)–(13) and (15)–(23) are satisfied along with $0 \leq \gamma \leq \gamma_{\max}$ and $e^T z \geq S_{\min}$. The nominal power flow solution (Tables VI and VII) provides an initial guess for this initialization procedure. Parameter $\gamma_{\max}$ is set to 0.9, a value close to but less than one, and $S_{\min}$ is set to 0.5, a small positive value, to avoid graph partitioning and/or trivial solutions. (One trivial/undesired solution is $\lambda = w_0, \mu_1 = e, \mu_2, \ldots, \mu_6, z = 0$; thus making the objective function zero.) This approach has been used to obtain solutions discussed in Sections III-A and B

We note that there are other ways to obtain feasible initial guesses for the optimization problem (26)–(41). One way features solving the simplified problem

$$\min_{\theta,V,z,\gamma,\mu_1,\ldots,\mu_6,\lambda} \quad \left\| e + \frac{\partial F}{\partial z}^T \lambda - \mu_1 + \mu_2 \right\|_2 \tag{48}$$

such that constraints (10)–(13) and (16)–(23) are satisfied along with $0 \leq \gamma \leq \gamma_{\max}, e^T\gamma \leq L_{\max}$ and $e^T z \geq S_{\min}$. The nominal power flow solution provides an initial guess for this initialization procedure. Random starting guesses have also produced solutions to (48).

REFERENCES

[1] Western Electricity Coordinating Council, Operating committee handbook, III-119, Revised, 2005.

[2] Western Electricity Coordinating Council, Operating Committee Handbook III-84, Revised, 2005.

[3] F. Alvarado, I. Dobson, and Y. Hu, "Computation of closest bifurcations in power systems," *IEEE Trans. Power Syst.*, vol. 9, no. 2, pp. 918–928, May 1994.

[4] J. Arroyo and F. Galiana, "On the solution of the bilevel programming formulation of the terrorist threat problem," *IEEE Trans. Power Syst.*, vol. 20, no. 2, pp. 789–797, May 2005.

[5] C. Cañizares, "Applications of optimization to voltage collapse analysis," in *Proc. IEEE/Power Eng. Soc. Summer Meeting, Panel Session: Optimization Techniques in Voltage Collapse Analysis*.

[6] C. Cañizares, "Conditions for saddle-node bifurcations in AC/DC power systems," *Int. J. Elect. Power Energy Syst.*, vol. 17, no. 1, pp. 61–68, 1995.

[7] C. Cañizares, W. Rosehart, A. Berizzi, and C. Bovo, "Comparison of voltage security constrained optimal power flow techniques," in *Proc. IEEE/Power Eng. Soc. Summer Meeting*, Vancouver, BC, Canada, Jul. 2001.

[8] Q. Chen and J. McCalley, "Identifying high risk $N-k$ contingencies for online security assessment," *IEEE Trans. Power Syst.*, vol. 20, no. 2, pp. 823–834, May 2005.

[9] C. L. DeMarco and J. Wassner, "A generalized eigenvalue perturbation approach to coherency," in *Proc. 4th IEEE Conf. Control Applications*, 1995, pp. 611–617.

[10] I. Dobson, "Observations on the geometry of saddle node bifurcation and voltage collapse in electrical power systems," *IEEE Trans. Circuits Syst. I: Fund. Theory Appl.*, vol. 39, no. 3, pp. 240–243, Mar. 1992.

[11] I. Dobson and L. Lu, "New methods for computing a closest saddle node bifurcation and worst case load power margin for voltage collapse," *IEEE Trans. Power Syst.*, vol. 8, no. 3, pp. 905–913, Aug. 1993.

[12] V. Donde, V. López, B. C. Lesieutre, A. Pinar, C. Yang, and J. Meza, "Identification of severe multiple contingencies in electric power networks," in *Proc. North Amer. Power Symp.*, Ames, IA, Oct. 2005.

[13] Z. Feng, V. Ajjarapu, and D. Maratukulam, "A practical minimum load shedding strategy to mitigate voltage collpase," *IEEE Trans. Power Syst.*, vol. 13, no. 4, pp. 1285–1291, Nov. 1998.

[14] A. Flueck and J. Dondeti, "A new continuation power flow tool for investigating the nonlinear effects of transmission branch parameter variations," *IEEE Trans. Power Syst.*, vol. 15, no. 1, pp. 223–227, Feb. 2000.
[15] P. E. Gill, W. Murray, and M. A. Saunders, "SNOPT: An SQP algorithm for large-scale constrained optimization," *SIAM J. Optim.*, vol. 12, no. 4, pp. 979–1006, 2002.
[16] S. Grijalva and P. W. Sauer, "A necessary condition for power flow Jacobian singularity based on branch complex flows," *IEEE Trans. Circuits Syst. I: Reg. Papers*, vol. 52, no. 7, pp. 1406–1413, Jul. 2005.
[17] S. Grijalva and P. W. Sauer, "Static collapse and topological cuts," in *Proc. 38th Annu. Hawaii Int. Conf. System Sciences*, Waikoloa, HI, Jan. 2005.
[18] T. He, S. Kolluri, S. Mandal, F. Galvan, and P. Rastgoufard, *Applied Mathematics for Restructured Electric Power Systems: Optimization, Control, and Computational Intelligence*. New York: Springer, 2005, ch. Identification of Weak Locations in Bulk Transmission Systems Using Voltage Stability Margin Index.
[19] I. Hiskens and R. Davy, "Exploring the power flow solution space boundary," *IEEE Trans. Power Syst.*, vol. 16, no. 3, pp. 389–395, Aug. 2001.
[20] B. Lesieutre and I. Hiskens, "Convexity of the set of feasible injections and revenue adequacy in FTR markets," *IEEE Trans. Power Syst.*, vol. 20, no. 4, pp. 1790–1798, Nov. 2005.
[21] T. J. Overbye, "A power flow measure for unsolvable cases," *IEEE Trans. Power Syst.*, vol. 9, no. 3, pp. 1359–1365, Aug. 1994.
[22] J. Salmeron, K. Wood, and R. Baldick, "Analysis of electric grid security under terrorist threat," *IEEE Trans. Power Syst.*, vol. 19, no. 2, pp. 905–912, May 2004.
[23] E. Scholtz, "Observer-based monitors and distributed wave controllers for electromechanical disturbances in power systems," Ph.D. dissertation, Massachusetts Inst. Technol., Cambridge, MA, 2004.
[24] S. Tong and K. Miu, "A network-based distributed slack bus model for DGs in unbalanced power flow studies," *IEEE Trans. Power Syst.*, vol. 20, no. 2, pp. 835–842, May 2005.
[25] AMPL: A Modeling Language for Mathematical Programming. [Online]. Available: http://www.ampl.com/.
[26] NEOS Server for Optimization. [Online]. Available: http://www-neos.mcs.anl.gov/.
[27] NEOS Guide: Optimization Software. [Online]. Available: http://www-fp.mcs.anl.gov/otc/Guide/SoftwareGuide/Blurbs/sqopt_snopt.html.
[28] Power System Test Case Archive. [Online]. Available: http://www.ee.washington.edu/research/pstca/.

Vaibhav Donde (S'01–M'04) received the B.E. degree in electrical engineering from V.J.T.I., Mumbai, India, in 1998 and the M.S. and Ph.D. degrees in electrical engineering from the University of Illinois at Urbana-Champaign in 2000 and 2004, respectively.

He is a Consulting R&D Engineer at ABB US Corporate Research Center, Raleigh NC. Prior to joining ABB, he had a postdoctoral appointment at Lawrence Berkeley National Laboratory, Berkeley, CA (2005–2006). He has worked with TATA Consulting Engineers, Mumbai (1998–1999). His technical interests include power system analysis, modeling and simulation, power distribution systems and automation, hybrid dynamical systems, and nonlinear control.

Vanessa López received the bachelor's degrees in mathematics from Rutgers, New Brunwick, NJ, and in computer information systems from the University of Puerto Rico, Río Piedras, and the Ph.D. degree in computer science from the University of Illinois at Urbana-Champaign, with a specialization in numerical analysis.

She is a Research Staff Member in the Mathematical Sciences Department at the IBM T.J. Watson Research Center, Yorktown Heights, NY. Prior to joining IBM, she had a postdoctoral appointment at the Computational Research Division, Lawrence Berkeley National Laboratory, Berkeley, CA.

Bernard Lesieutre (S'86–M'93) received the B.S., M.S., and Ph.D. degrees in electrical engineering from the University of Illinois at Urbana-Champaign in 1986, 1988, and 1993, respectively.

He is an Associate Professor at University of Wisconsin-Madison. Prior to this appointment, he was a Staff Scientist at the Ernest Orlando Lawrence Berkeley National Laboratory, Berkeley, CA. He served on the faculty of the Massachusetts Institute of Technology, Cambridge, as Assistant Professor and then Associate Professor of electrical engineering from 1993 to 2001. He has also held Visiting Associate Professor appointments at Caltech and Cornell University. His research interests include the modeling, monitoring, and analysis of electric power systems and electric energy markets.

Ali Pınar (M'04) received the B.S. and M.S. degrees in computer engineering from Bilkent University, Ankara, Turkey, and the Ph.D. degree in computer science from University of Illinois at Urbana-Champaign.

He has been working at Lawrence Berkeley National Laboratory, Berkeley, CA, since 2001. His research interests include combinatorial scientific computing, combinatorial algorithms, parallel algorithms, data analysis, and electric power systems.

Dr. Pínar is a member of SIAM, ACM, and the IEEE Computer Society.

Chao Yang received the Ph.D. degree in computational science and engineering from Rice University, Houston, TX, in 1998.

He is currently a staff computer scientist in the Computational Research Division at Lawrence Berkeley National Laboratory (LBNL), Berkeley, CA. His research interests include large-scale scientific computing, numerical optimization, and image processing. He is a coauthor of the ARPACK software, widely used for large-scale eigenvalue computation. After receiving the Ph.D. degree , he worked briefly at NEC Systems Laboratory, Woodlands, TX. He was with Oak Ridge National Laboratory from 1999 to 2000. He joined LBNL in 2000. From 2002 to 2003, he was a senior scientist at ILOG, Mountain View, CA.

In 1999, Dr. Yang was awarded the Householder fellowship in scientific computing by Oak Ridge National Laboratory.

Juan Meza received the B.S. and M.S. degrees in electrical engineering and the M.S and Ph.D. degrees in computational mathematics from Rice University, Houston, TX, in 1978, 1979, and 1986, respectively.

He is currently the Department Head of High Performance Computing Research at Lawrence Berkeley National Laboratory (LBNL), Berkeley, CA. This department focuses on research in scientific data management, visualization, numerical algorithms, and computational sciences and engineering. Prior to joining LBNL, he was a Distinguished Member of the Technical Staff at Sandia National Labs, Albuquerque, NM. His current research interests include nonlinear optimization with an emphasis on parallel methods for simulation-based optimization. He has also worked on various scientific and engineering applications, including methods for electronic structure calculations for nanoscience applications, mixed integer nonlinear programming methods for detecting vulnerabilities in electric power grids, optimization methods for molecular conformation problems, optimal design of chemical vapor deposition furnaces, and semiconductor device modeling.

Dr. Meza has served on numerous committees, including the DOE Advanced Scientific Computing Advisory Committee, SIAM Board of Trustees, IMA Board of Governors, and MSRI Human Resources Advisory Committee.